Molecular Dynamics Simulations of Rapid Hydrogen Production from Water Using Aluminum Clusters as Catalyzers

Fuyuki Shimojo,[1,2] Satoshi Ohmura,[1,2] Rajiv K. Kalia,[1] Aiichiro Nakano,[1] and Priya Vashishta[1]

[1]*Collaboratory for Advanced Computing and Simulations, Department of Computer Science, Department of Physics & Astronomy, Department of Chemical Engineering & Materials Science, University of Southern California, Los Angeles, California 90089-0242, USA*

[2]*Department of Physics, Kumamoto University, Kumamoto 860-8555, Japan*

(Received 1 December 2009; published 26 March 2010)

Hydrogen production by metal particles in water could provide a renewable energy cycle, if its reaction kinetics is accelerated. Here, *ab initio* molecular dynamics simulation reveals rapid hydrogen production from water by a cluster (or superatom) consisting of a magic number of aluminum atoms, Al_n (for instance, $n = 12$ or 17). We find a low activation-barrier mechanism, in which a pair of Lewis-acid and base sites on the Al_n surface preferentially catalyzes hydrogen production. This reaction is immensely assisted by rapid proton transport in water via a chain of hydrogen-bond switching events similar to the Grotthuss mechanism, which converts hydroxide ions to water molecules at the Lewis-acid sites and supplies hydrogen atoms at the Lewis-base sites.

DOI: 10.1103/PhysRevLett.104.126102 PACS numbers: 82.45.Jn, 71.15.Pd, 82.30.−b

Hydrogen production by metal particles in water could provide a renewable energy cycle [1–3] to address the global energy problem [4]. Unfortunately, conventional metal-water reaction kinetics is not fast enough to make it viable [5]. This Letter suggests a possible nanotechnology-based solution to this problem. Chemical reactivity at the nanoscale differs drastically from its macroscopic counterpart [6,7]. For example, flame propagation speeds for metallic nanoparticles embedded in oxidizers are accelerated to km/s, compared with cm/s in the case of micron-size particles [8]. Such rapid nanoreaction cannot be explained by conventional mechanisms based on mass diffusion of reactants, and thus various mechanisms for enhanced nanoenergetic reactions have been proposed [8–10]. Furthermore, metal nanoclusters possess catalytic behaviors that are distinct from larger particles [11,12]. A remarkable example is size-selective reactivity of Al clusters with water [13], where an anion of Al cluster, Al_n^- (for instance, $n = 12$ or 17), reacts strongly with water. This raises hope that these Al "superatoms" [13,14] may be tailored to accelerate hydrogen production from water, which remains to be demonstrated either experimentally or theoretically.

Here, we perform *ab initio* molecular dynamics (MD) simulations on a parallel computer (see the supplementary material [15]) to reveal rapid hydrogen production by Al_n ($n = 12$ and 17) in bulk water, which is assisted by rapid proton transport [16,17] via a chain of hydrogen-bond switching events similar to the Grotthuss mechanism [18–20]. In our simulation at room temperature (300 K), several water molecules bond to the Al clusters—6 H_2O and 5 H_2O in the Al_{17} and Al_{12} cases, respectively. Formation of these Al-O bonds enhances the Lewis-base character of Al atoms that are not connected to the water molecules, thereby preventing further bonding of water molecules to the Al clusters. Dissociation of water molecules is not observed within the limited simulation time (several ps) at this temperature. Even when the temperature is raised to 500 K, still no water molecule dissociates, though the shape of the Al_{12} cluster is deformed. In contrast, the Al_{17} cluster is stable in water even at 1000 K as shown in Fig. 1(a), and we mainly discuss Al_{17} results in the following. The different stability of the two clusters originates from the symmetry of their shapes. The Al_{17} cluster is highly symmetric with closely packed atoms,

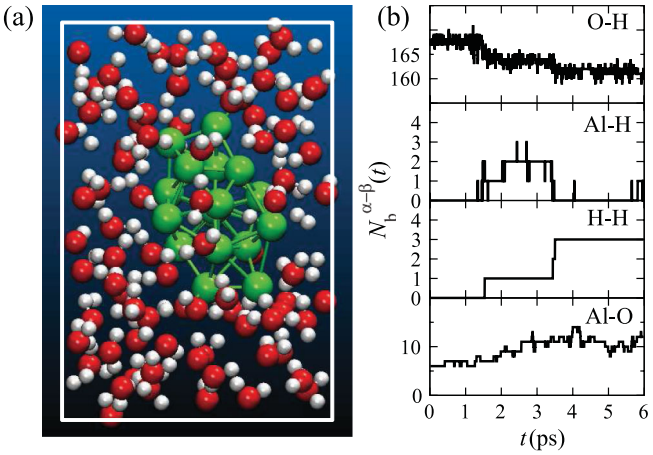

FIG. 1 (color). (a) Snapshot of the Al_{17} + water system, where green, red, and white spheres represent aluminum, oxygen, and hydrogen atoms, respectively. (b) Time evolution of the number of chemical bonds $N_b^{\alpha-\beta}(t)$. Two atoms are considered bonded when their distance is less than a cutoff distance R_c during a prescribed bond lifetime 12 fs [16], where R_c is 1.3, 2.0, 1.0, and 2.4 Å for O-H, Al-H, H-H, and Al-O pairs, respectively.

while Al_{12} has low symmetry with a concave shape [13]. The atomistic process of hydrogen production is successfully observed in MD simulation for Al_{17} in water at 1000 K. In total, three hydrogen molecules are produced within 6 ps [Fig. 1(b)] [21]. The overall reaction involves three steps that are described in detail below.

To find the mechanism of hydrogen production, Fig. 2 shows the time evolution of bond-overlap populations $O_{ij}(t)$ (see the supplementary material [15]) between atomic pairs (i, j) of interest, along with snapshots of atomic configurations. At 0 fs, one H atom labeled "H1" bonds to an Al atom labeled "Al1", and one water molecule consisting of H2, H3, and O1 bonds to another Al atom labeled "Al3". In Fig. 2(a), $O_{ij}(t)$ for H1-Al1 and O1-Al3, as well as those for O1-H2 and O1-H3 within the water molecule, take finite values at 0 fs, signifying chemical bonds between these atoms. At 25 fs, $O_{\mathrm{H1\text{-}H2}}(t)$ and $O_{\mathrm{H1\text{-}Al2}}(t)$ begin to increase (Al2 is an Al atom adjacent to Al3), and at the same time $O_{\mathrm{H1\text{-}Al1}}(t)$ decreases rapidly. In the snapshot at 36 fs in Fig. 2(b), H1 atom bonds partially to those three (H2, Al1, and Al2) atoms. While $O_{\mathrm{H1\text{-}Al2}}(t)$ decreases after 40 fs, $O_{\mathrm{H1\text{-}H2}}(t)$ continues to increase and maintains a quite large value ~0.8 after 70 fs, i.e., a hydrogen molecule (H1-H2) is formed as shown in the snapshots at 56 and 122 fs in Fig. 2(b) (supplementary movie S1 shows this hydrogen-production process [15]). The chemical bond between O1 and Al3 strengthens as $O_{\mathrm{O1\text{-}Al3}}(t)$ exceeds 0.8, which is accompanied by the breakage of one of the O-H bonds (O1-H2) in the water molecule, leaving a hydroxide ion (O1-H3) at 56 fs. Subsequently, the OH group turns into an H_2O molecule by the Grotthuss mechanism [18–20] with another hydrogen atom (H4) supplied by surrounding water molecules [see the snapshot at 122 fs in Fig. 2(b)]. $O_{\mathrm{O1\text{-}H4}}(t)$ increases gradually after 70 fs, and simultaneously $O_{\mathrm{O1\text{-}Al3}}(t)$ decreases. This hydrogen-production reaction is thus summarized as

$$\mathrm{Al\text{-}OH_2 + Al\text{-}H \rightarrow Al\text{-}OH + Al + H_2}. \qquad (1)$$

As mentioned above, it is notable that the Al-OH product of this reaction thermally fluctuates back to $Al\text{-}OH_2$, the mechanism of which will be elucidated below.

In order to estimate the rate of the hydrogen-production reaction, Eq. (1), we calculate the energy profile along the corresponding reaction path using the nudged elastic band (NEB) method (see the supplementary material [15]) [22]. From the result shown in Fig. 2(c), the activation energy is estimated to be $\Delta = 0.1$ eV. We also study the finite-temperature effect by calculating the activation free energy (see the supplementary material [15]) [23], which gives a nearly identical value, $\Delta = 0.08$ eV, at 300 K (supplementary material Fig. S1(a) [15]). The corresponding reaction rate is estimated as $k_{\mathrm{H_2}} = (k_B T/h)\exp(-\Delta/k_B T) = 10^{11}\ \mathrm{s}^{-1}$ at room temperature ($T = 300$ K) according to the transition state theory [24], where k_B is the Boltzmann

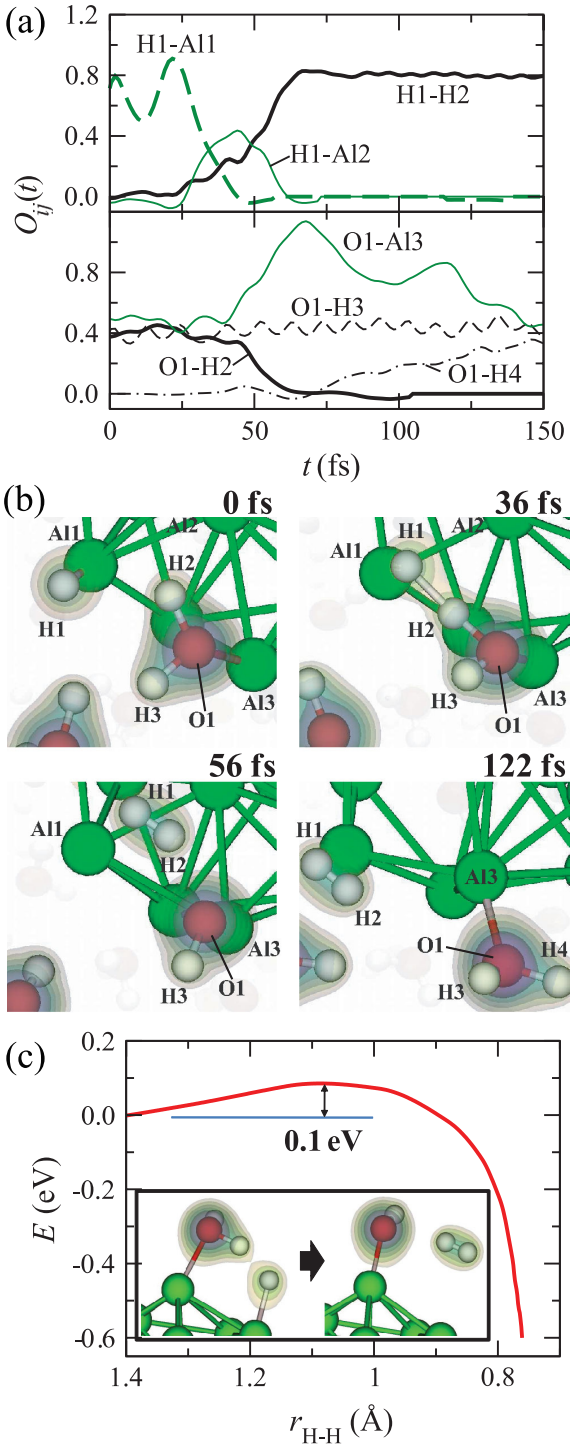

FIG. 2 (color). (a) Time evolution of bond-overlap populations $O_{ij}(t)$ associated with atoms labeled in the center panel. (b) Atomic configurations at time $t = 0$, 36, 56, and 112 fs, where white, red, and green spheres represent H, O, and Al atoms, respectively. Here, the time origin is taken as $t = 1.48$ ps in Fig. 1. (c) Energy profile along the reaction path of molecular hydrogen production, $\mathrm{Al\text{-}OH_2 + Al\text{-}H \rightarrow Al\text{-}OH + Al + H_2}$, as a function of the distance between the two hydrogen atoms that form a hydrogen molecule, obtained by nudged elastic band calculations. The distribution of the electron density larger than 0.05 a.u. is shown by contour surfaces.

constant and h is the Planck constant. This reaction is much faster than a previously studied mechanism (see the rate-limiting reaction labeled "*I*" in Fig. 4 of Ref. [13]), i.e., formation of a hydrogen molecule from two hydrogen atoms on an Al cluster, which has a much higher activation free energy, 0.9 eV [see the red curve in Fig. S1(b)]. We have also considered several other mechanisms for Al-water interaction [Figs. S1(b) and S2], which all have much higher activation barriers than that for Eq. (1).

In order to understand how the Grotthuss mechanism assists the production of hydrogen molecules, Fig. 3(a) shows atomic configurations for the adsorption of a hydrogen atom on the Al cluster during the MD simulation. The reaction begins with the dissociation of an H_2O molecule bonding to an Al atom [the magenta circle in Fig. 3(a)], as one of its hydrogen atoms moves toward a neighboring H_2O molecule to form a hydronium ion (H_3O^+). This is followed by a chain of hydrogen-bond switching events [denoted by yellow arrows in Fig. 3(a)] that involves a total of four H_2O molecules, and finally a hydrogen atom bonds to an Al atom after 190 fs [the cyan circle in Fig. 3(a)]. This proton transfer is induced by the Lewis-acid-base characters of the participating Al atoms [13]. (Similar phenomena were observed in water with hydrogen-bonded acid-base complexes [25] or charged solutes [26].)

To estimate the energy barrier for this process, we first calculate the energy profile along the reaction path for the production of a hydroxide group and a hydrogen atom on the Al cluster,

$$\text{Al-OH}_2 + m\text{H}_2\text{O} + \text{Al}' \rightarrow \text{Al-OH} + m\text{H}_2\text{O} + \text{Al}'\text{-H}, \tag{2}$$

where $m = 3$ for the process observed in the MD simulation shown in Fig. 3(a). (Figure S3 shows activation barriers for different values of m.) In Eq. (2), Al and Al$'$ denote the aluminum atoms with Lewis-acid and base characters, respectively, involved in the reaction. The result is shown in Fig. 3(b), from which the activation energy is estimated to be $\Delta = 0.3$ eV. The rate of this reaction at room temperature is $k_1 = (k_BT/h)\exp(-\Delta/k_BT) = 10^7\ \text{s}^{-1}$.

In the process shown in Fig. 3(a), the Al-OH product of Eq. (2) is quickly converted back to Al-H_2O again by the Grotthuss mechanism, which involves a third Al atom (denoted as Al$''$) with an adsorbed water molecule:

$$\text{Al-OH} + m\text{H}_2\text{O} + \text{Al}''\text{-OH}_2 \rightarrow \text{Al-OH}_2 + m\text{H}_2\text{O} + \text{Al}''\text{-OH}. \tag{3}$$

The activation energy of this reaction [Fig. 3(c)] is 0.03 eV with the corresponding rate $k_2 = 10^{12}\ \text{s}^{-1} \gg k_1$ at 300 K. The combined reactions, Eqs. (2) and (3), have the rate of $k_H = \min(k_1, k_2) = 10^7\ \text{s}^{-1}$, and their end products, Al-OH_2 + Al$'$-H, become the reactants of the hydrogen-production reaction, Eq. (1) [27].

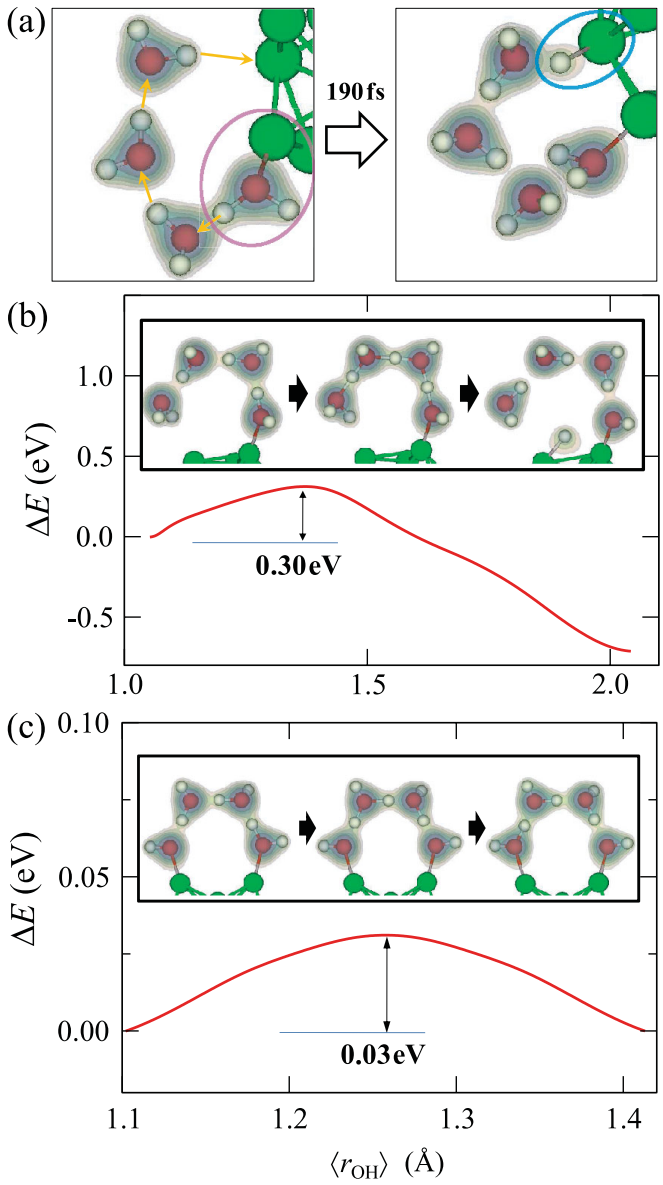

FIG. 3 (color). (a) Adsorption of a hydrogen atom on the Al cluster through the Grotthuss mechanism observed in MD simulation. (b) Energy profile along the reaction path for the production of a hydroxide ion and a hydrogen atom, Al + $4H_2O$ + Al → Al-OH + $3H_2O$ + Al-H, obtained by nudged elastic band calculations. (c) Energy profile along the reaction, Al-OH + $2H_2O$ + Al-OH_2 → Al-OH_2 + $2H_2O$ + Al-OH, obtained by nudged elastic band calculations. Here, $\langle r_{OH}\rangle$ is the average length of OH bonds, which are broken in the reaction. The distribution of the electron density larger than 0.05 a.u. is shown by contour surfaces.

The overall mechanism of H_2 production by Al_{17} in water is summarized in Fig. 4. First, an oxygen atom in a water molecule bonds to an Al atom with the Lewis-acidic character [Fig. 4(a)]. This enhances the Lewis-basic character of surrounding Al atoms [13], and in turn a hydrogen atom is generated at a surrounding Lewis-base site assisted by rapid proton transport as in Eqs. (2) and (3) [Fig. 4(c)].

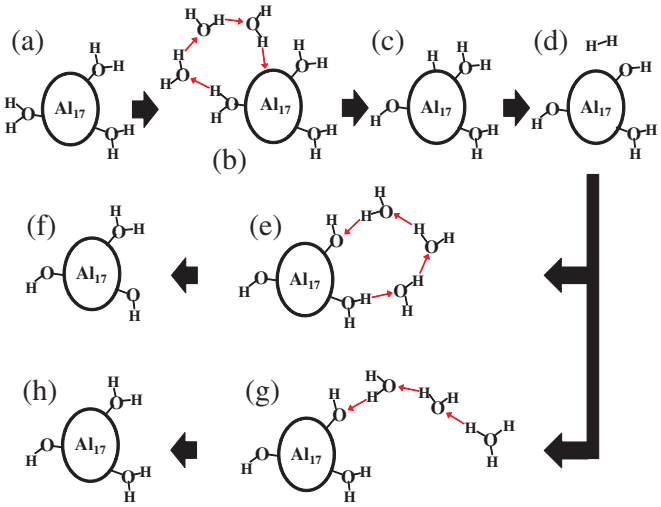

FIG. 4 (color). Schematic diagram of reaction processes on an Al cluster. The production process of a hydrogen molecule (a)–(d) and the recovery process of a water molecule (e)–(h) on the surface of the Al cluster.

Although it is hard for the water molecule to dissociate by itself, the Grotthuss mechanism [Fig. 4(b)] greatly reduces the activation barrier for the dissociation. Finally, a hydrogen molecule is produced from the water molecule and the hydrogen atom on the Al cluster as in Eq. (1), which has a lower activation barrier than that for hydrogen-atom generation [Fig. 4(d)]. Since the resulting hydroxide ion has a strong Lewis-base character and returns to a water molecule again through the Grotthuss mechanism [Figs. 4(f) and 4(h)], hydrogen production can continue, especially in acidic conditions. The reactions found in our simulations are very rapid with the rate-limiting step of $k_H = 10^7\ s^{-1}$ at 300 K, which is an enormous enhancement of reaction rates compared with those of existing Al-particle-based hydrogen-production methods [28]. Under acidic conditions, these superatoms can continuously produce hydrogen molecules at room temperature. Thus, Al-superatom-based hydrogen production from water is highly promising, only if the superatoms are mass produced and acidic conditions are maintained. Furthermore, the reaction specificity and efficiency achieved by superatoms and autocatalytic behavior of water presented here may be applicable to much broader applications, e.g., direct splitting of water using photocatalysts [29–31].

This work was supported by DOE-BES Grant No. DE-FG02-04ER46130. F. S. acknowledges support by a Grant-in-Aid for Scientific Research on Priority Area, "Nanoionics (439)" from the MEXT, Japan. Simulations were performed at the University of Southern California Research Computing Facility.

[1] A. Steinfeld, Solar Energy **78**, 603 (2005).
[2] T. Yabe *et al.*, Appl. Phys. Lett. **89**, 261107 (2006).
[3] Exothermic reactions between metal and water produce hydrogen, followed by endothermic reduction of metal-oxide products to regenerate metal fuel assisted by solar energy, e.g., using solar-powered lasers.
[4] N. S. Lewis, Science **315**, 798 (2007).
[5] J. Petrovic and G. Thomas, *Reaction of Aluminum with Water to Produce Hydrogen* (U.S. Department of Energy, Washington, DC, 2008).
[6] Y. Huang *et al.*, Combust. Flame **156**, 5 (2009).
[7] Y. Q. Yang *et al.*, Appl. Phys. Lett. **85**, 1493 (2004).
[8] V. I. Levitas *et al.*, Appl. Phys. Lett. **89**, 071909 (2006).
[9] F. Shimojo *et al.*, Appl. Phys. Lett. **95**, 043114 (2009).
[10] S. K. R. S. Sankaranarayanan, E. Kaxiras, and S. Ramanathan, Phys. Rev. Lett. **102**, 095504 (2009).
[11] M. Valden, X. Lai, and D. W. Goodman, Science **281**, 1647 (1998).
[12] B. Yoon *et al.*, Science **307**, 403 (2005).
[13] P. J. Roach *et al.*, Science **323**, 492 (2009).
[14] D. E. Bergeron *et al.*, Science **304**, 84 (2004).
[15] See supplementary material at http://link.aps.org/supplemental/10.1103/PhysRevLett.104.126102 for simulation details.
[16] C. J. Wu *et al.*, Nature Chem. **1**, 57 (2009).
[17] E. Vöhringer-Martinez *et al.*, Science **315**, 497 (2007).
[18] N. Agmon, Chem. Phys. Lett. **244**, 456 (1995).
[19] D. Marx *et al.*, Nature (London) **397**, 601 (1999).
[20] H. S. Kato *et al.*, J. Phys. Chem. C **112**, 12879 (2008).
[21] As a reference, we have simulated water without an Al cluster at the same temperature. This simulation did not produce any hydrogen molecule.
[22] G. Henkelman and H. Jonsson, J. Chem. Phys. **113**, 9978 (2000).
[23] K. C. Hass *et al.*, Science **282**, 265 (1998).
[24] D. G. Truhlar, B. C. Garrett, and S. J. Klippenstein, J. Phys. Chem. **100**, 12771 (1996).
[25] M. Rini *et al.*, Science **301**, 349 (2003).
[26] P. L. Geissler *et al.*, Science **291**, 2121 (2001).
[27] It should be noted that bulk water surrounding the Al cluster provides a number of alternative reaction pathways for the production of the reactants in Eq. (1). For example, a hydrogen molecule could instead be produced from Al″-OH_2 and Al′-H, if Al′ and Al″ are spatially proximate. In this case, the reaction rate of producing Al″-OH_2 + Al′-H is $k_1 = 10^7\ s^{-1}$, which is the same as k_H. Also, Al-OH could be converted to Al-OH_2 by reacting with a hydronium ion in water through the Grotthuss mechanism, Al-OH + mH_2O + $H_3O^+ \rightarrow$ Al-OH_2 + $(m + 1)H_2O$, especially if the water is in an acidic condition.
[28] H. Z. Wang *et al.*, Renew. Sustain. Energ. Rev. **13**, 845 (2009).
[29] Z. G. Zou *et al.*, Nature (London) **414**, 625 (2001).
[30] K. Maeda *et al.*, Nature (London) **440**, 295 (2006).
[31] M. W. Kanan and D. G. Nocera, Science **321**, 1072 (2008).